

## Distributions of Avalanches in Martensitic Transformations

Eduard Vives, Jordi Ortín, Lluís Mañosa, Ismael Ràfols, Ramon Pérez-Magrané, and Antoni Planes

*Departament d'Estructura i Constituents de la Matèria, Facultat de Física, Universitat de Barcelona,  
Diagonal 647, E-08028 Barcelona, Catalonia, Spain*

(Received 30 July 1993)

An experimental study of the acoustic emission generated during a martensitic transformation is presented. A statistical analysis of the amplitude and lifetime of a large number of signals has revealed power-law behavior for both magnitudes. The exponents of these distributions have been evaluated and, through independent measurements of the statistical lifetime to amplitude dependence, we have checked the scaling relation between the exponents. Our results are discussed in terms of current ideas on avalanche dynamics.

PACS numbers: 64.60.Ht, 05.40.+j, 64.60.My, 81.30.Kf

The study of externally driven complex dissipative systems with spatial and temporal degrees of freedom has received major interest after the work of Bak, Tang, and Wiesenfeld [1]. They suggest that these systems naturally evolve into a critical state characterized by avalanches with no intrinsic time or length scale: This behavior is called self-organized criticality (SOC). The absence of characteristic scales results in power-law distributions for both size and duration of the avalanches. The search for real physical systems exhibiting SOC has been a challenge in recent years. Experimental data displaying power laws have been reported for earthquakes [2], rearrangement of magnetic domains [3], Barkhausen effect in amorphous alloys [4], avalanches in granular materials [5], and acoustic emission from volcanic rocks [6] and from fracture processes [7]. Though many of these experiments have been interpreted in the framework of Bak's ideas, the nonuniqueness of SOC models has also been pointed out.

The purpose of this Letter is to show the absence of characteristic scales in the distribution of avalanches in thermally induced martensitic transformations. A martensitic transformation is a diffusionless first order phase transition where the lattice distortion is mainly described by a homogeneous shear [8]. It can be induced either by changing the temperature or by an external applied stress. Many metals and alloys with a bcc structure exhibit this transition on cooling from the high temperature phase towards a low temperature close-packed structure. As a consequence of the significant change in shape of the unit cell, the nucleation of domains of the low temperature phase modifies the internal strain field of the system. The strain energy can be stored in the lattice elastically (the transition is called thermoelastic for this reason) and blocks subsequent growth of the new phase completely, leaving the system in a metastable two-phase state; additional undercooling is then needed for the transition to proceed. As a consequence, the transition is athermal: Temperature acts as an external field and thermal fluctuations do not play any relevant role. The transition takes place as a sequence of avalanches between metasta-

ble states in a broad temperature range, each avalanche corresponding to the motion of one (or several) interface. This motion generates elastic waves in the ultrasonic range [acoustic emission (AE)] which travel through the material and can be detected by appropriate transducers [9]. The amplitude ( $A$ ) and the duration ( $T$ ) of an AE signal provide information about the size and the lifetime of an avalanche [10]. This acoustic emission has many similarities with seismic waves generated during an earthquake, but at a microscopic scale. Moreover, the underlying physical mechanism is a shear in both cases.

We have measured the AE generated during the martensitic transformation of a Cu-Zn-Al single crystal (Cu-13.7 Zn-17.0 Al at. %). On cooling, the transition starts at  $M_s=299$  K and finishes at  $M_f=268$  K. The transition on heating displays hysteresis, starting at  $A_s=278$  K and finishing at  $A_f=308$  K. We have performed several heating and cooling cycles before starting our measurements in order to ensure a very good reproducibility of the transformation. Heating and cooling are performed using a computer controlled system which allows control of the sample temperature with an accuracy better than 0.1 K. AE signals are detected by a piezoelectric transducer, acoustically coupled to the surface of the sample. These signals are amplified and displayed on the screen of a digitizing oscilloscope, and sent to a multichannel analyzer to obtain the amplitude and time distributions. For the latter measurements the signals pass through a gate circuit and a time-to-voltage converter before being sent to the multichannel analyzer. A detailed description of the experimental setup will be given elsewhere [11].

A typical signal is presented in Fig. 1, together with the gate signal used to measure its duration  $T$ . The distribution of the amplitudes is shown in Fig. 2 for cooling and heating rates of  $1 \text{ K min}^{-1}$  [12]. A number of experiments have been performed at four different amplifications (40, 45, 50, and 55 dB). For each experiment a log-log plot exhibits a linear behavior in a broad region of amplitudes. The slope of the linear region has been found to be the same within experimental accuracy for the four

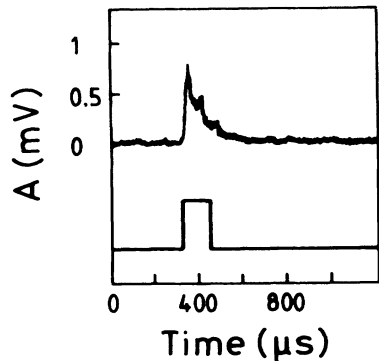


FIG. 1. Typical AE signal detected with a piezoelectric transducer during a martensitic transformation of a Cu-Zn-Al alloy. The curve below shows the signal generated by an electronic gate used to measure the duration of the AE signal.

different amplifications used and has enabled us to overlap the experimental data after a proper renormalization. By this procedure we obtain reliable data expanding over about 2 decades in amplitude. The breakdown of the power-law behavior [ $N(A) \sim A^{-\alpha}$ ] is due at low amplitudes to the background noise and to the detection threshold of the multichannel analyzer and at high amplitudes to the amplifier cutoff. A slightly different behavior is obtained for cooling and heating. Best fits to the data

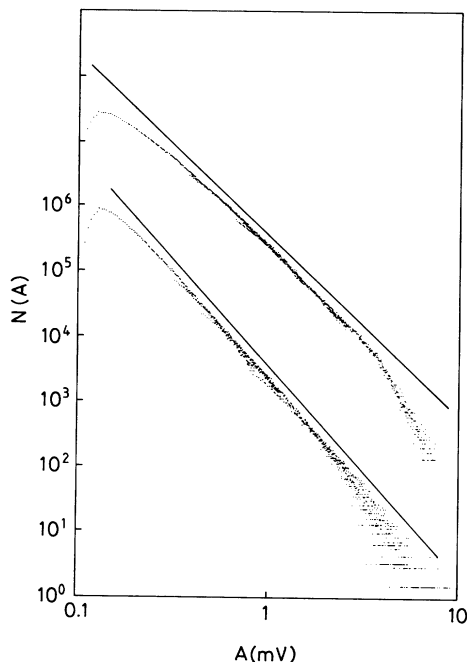


FIG. 2. Log-log plot of the amplitude distribution of AE signals for heating (top) and cooling (bottom) processes. The curves have been plotted after overlapping data obtained with four amplifications (40, 45, 50, and 55 dB). The straight lines are fits to the linear regime with slopes  $\alpha=3.2$  and  $\alpha=2.8$ . The vertical scale has arbitrary units, proportional to the number of counts.

give  $\alpha=3.2 \pm 0.2$  for cooling and  $\alpha=2.8 \pm 0.2$  for heating. Indeed, different behavior between the AE detected during cooling and heating was already reported for martensitic transformations and has been accounted for by a different dissipative mechanism in the growth and shrinkage of domains [13].

Figure 3 shows the time distribution of AE signals for heating and cooling. These distributions are less accurate than the amplitude ones; in addition to the previously mentioned experimental limitations, the resonant behavior of the transducer may also have an influence on time distributions (mainly at short times). In order to estimate this effect, we have performed some measurements with transducers having different characteristics, which have shown that reliable data are obtained for times longer than 25  $\mu\text{s}$ . The log-log plots show a power-law regime [ $N(T) \sim T^{-\tau}$ ] extending over 1 decade. A linear fit on this region renders values for the exponent  $\tau=1.6 \pm 0.3$  for both heating and cooling.

A power-law behavior of the amplitude and time distributions leads to the statistical relationship  $A(T) \sim T^{-x}$  between amplitude and duration;  $x$  is a dynamical exponent that must obey the following simple scaling relation:

$$(\alpha - 1)x = \tau - 1, \quad (1)$$

For  $\alpha=3.0 \pm 0.2$  and  $\tau=1.6 \pm 0.3$  one gets a dynamical exponent  $x=0.3 \pm 0.2$ . To check the consistency of this scaling law, we have acquired a large number (over 500) of AE signals with a high-speed digitizing oscilloscope, recording simultaneously the amplitude and duration of each signal. This analysis has been restricted to those regions (in time and amplitude) where the two distributions display a power-law behavior. In Fig. 4(a) we show the amplitude ( $A$ ) versus time ( $T$ ) for the AE

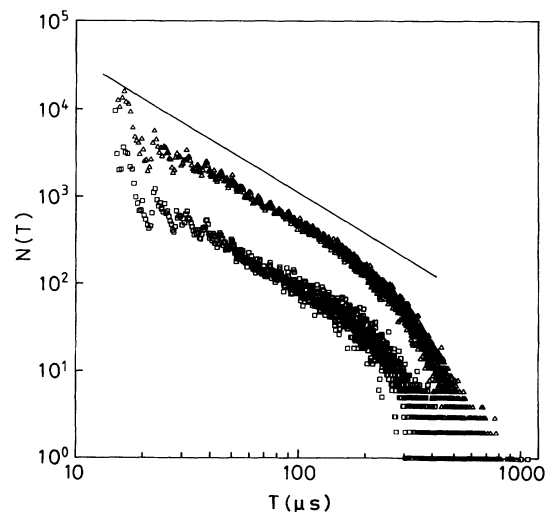


FIG. 3. Log-log plot of the time distribution of AE signals for heating (top) and cooling (bottom) processes, obtained at 55 dB. The straight line shows a power law with exponent  $\tau=1.6$ .

signals acquired at different stages in the transformation. The reliability of the statistical sample is checked through computation of the marginal amplitude and time distributions shown in Figs. 4(b) and 4(c), respectively. These distributions conform to a power law with the same exponents obtained previously via multichannel measurements. A rough estimation of the exponent  $x$  is obtained by performing a least-squares fit to the raw data, rendering  $x=0.48$ . This value is slightly larger than the one predicted ( $x=0.3$ ), but still within the experimental error. A better approach to the statistical relation between  $A$  and  $T$  is obtained with a density map of the data points [also shown in Fig. 4(a)] [14]. We have compared the line following the crest of the distribution to the  $x=0.3$  power law predicted from Eq. (1). It is apparent from the figure that both lines are quite close, and hence there is a good agreement between experiments and Eq. (1). Maximum discrepancy is observed for low values of amplitude and time.

The exponents found for martensitic transformations compare well with previously published values in other systems: A value  $\alpha \sim 3$  [2,15] has been found from the

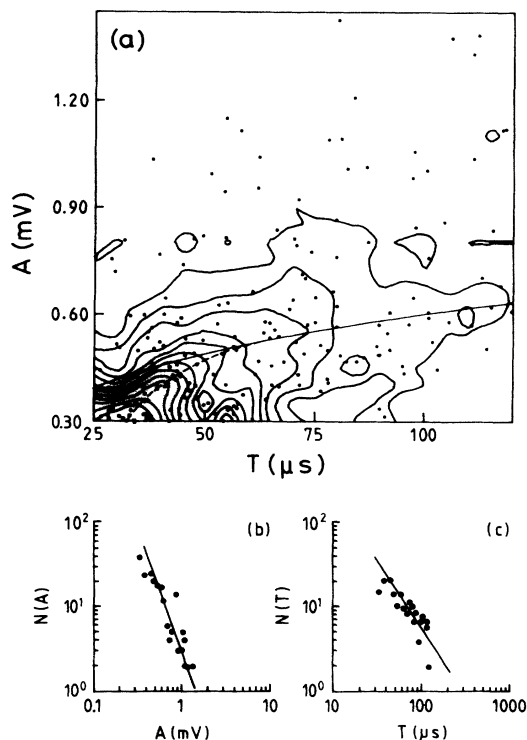


FIG. 4. (a) Amplitude ( $A$ ) vs duration ( $T$ ) of recorded AE signals. Contour levels of the density map obtained from the data points ( $\bullet$ ) are shown for increasing densities, from 0.5 up to 6 mean counts per grid cell. The continuous line represents a power-law behavior with exponent  $x=0.3$ . The dashed line indicates the crest of the density map. (b) and (c) are the marginal amplitude and time distributions from the same data points in log-log scale. The straight lines show power laws with exponents  $\alpha=3$  and  $\tau=1.6$ .

energy distribution of earthquakes. This value has also been obtained theoretically using a mean-field-like approach [16], which is supposed to be valid [17] for system dimension  $d \geq d_c = 3$  when long-range interactions are present in the system. Values  $\tau \sim 1.2$  and  $\sim 1.59$  have been found for the time distribution of avalanches in volcanic rocks [6,18] and in the reorientation of magnetic domains [4], respectively.

At this point, it is worth mentioning that a recent revision of experimental data of reorientation of magnetic domains and several computer simulations [19,20] have shown that systems evolving by avalanches can alternatively display power-law distributions damped by an exponential term. Our results, however, seem to be consistent with a pure power-law behavior up to the cutoff imposed by the limitations of our experimental setup: Although the deviation of our time distribution from a power law at large times (that we would attribute to finite size effects) could be indicative of a damping prefactor, we clearly observe that the linear regime in the log-log amplitude distributions shifts towards larger amplitudes at increasing amplifications.

In a recent paper, Sethna *et al.* [21] propose a spin model for disorder-driven first-order phase transitions which includes the essential ingredients to account for the elastic interactions between martensite domains, i.e., a ferromagnetic interaction, favoring the parallel orientation of the domains, and a random field acting on each domain, to mimic its interaction with structural defects (impurities, dislocations, ...). The model is particularly suitable for reproducing the properties of the hysteresis cycles observed when the transformation is driven either thermally or by an external applied stress [22]. By changing the degree of disorder in the system the authors have discovered a phase transition between a region (low disorder) where the hysteresis cycle is dominated by a single infinite avalanche (turning almost all spins at once) and a region (high disorder) with a hysteresis cycle made up as a sequence of tiny avalanches. For a critical value of the disorder, the system evolves through a sequence of avalanches of all sizes with no characteristic length scale. In connection with this model, the fact that we have found a power-law distribution of avalanches in our crystal would suggest that, after an initial number of cycles, the degree of disorder in the system self-organizes into this critical state; i.e., the hysteresis cycle evolves with the number of cycles until a final attractor is reached, which corresponds to the critical value of disorder. This picture is supported by the following two experimental observations [23]: First, the initial hysteresis cycle is strongly dependent upon the thermal treatment (which controls the quenched-in disorder) of the sample. For samples slowly cooled from a high temperature (over 1000 K), defect concentration is very low and the cycle displays very large avalanches, while for samples directly quenched (higher concentration of defects) the cycle displays only tiny avalanches. Second, after a number of cycles the

hysteresis cycle evolves towards a behavior quite independent of the initial thermal treatment. Systematic measurements of AE distribution as a function of cycling are now under course.

Since the emergence of the SOC ideas [1] a renewed interest has arisen in alternative attempts to explain the occurrence of power-law distributions of avalanches in complex systems. These include theories based on (i) the extremal dynamics of activated processes [24], (ii) the sweeping of an instability mechanism [25], and (iii) the existence of log-normal distributions arising from mechanisms of a multiplicative nature in complex systems [26]. These theories, and the SOC concept itself, are all of a very general nature and share the property that they lead to power-law distributions, equivalent to the ones obtained in our experiments. Moreover, the different approaches associate power-law distributions to fractal geometries in the system. Indeed, self-similarity in martensite domains has already been reported for iron based alloys [27]. For Cu-Zn-Al, self-similar surface structures (needle shaped) have been observed by optical microscopy in spatial scales from (at least) micrometers up to millimeters [28]. In addition, a correlation between the detection of AE signals and the appearance and growth of such transformed domains has been observed [29]. Each AE burst is associated with the appearance or advance of one or several interfaces (avalanche) in the material. Its square amplitude ( $A^2$ ) and duration ( $T$ ) are related, respectively, to the energy release and duration of each avalanche.

To conclude, we have shown the absence of intrinsic scales in the dynamics of martensitic transformations. We have independently measured two exponents  $\alpha$  and  $\tau$ , and checked that the value predicted for the exponent  $x$  based on scaling arguments is also consistent with experimental data. We suggest that the defect structure in the system reorganizes during cycling in such a way that the hysteresis cycles evolve towards a final attractor, characterized by avalanches with no characteristic temporal and spatial scales.

We are grateful to Professor P.-A. Lindgård for calling our attention to the possibility of finding SOC in martensitic transformations. We acknowledge the Comisión Interministerial de Ciencia y Tecnología (Spain) for financial support (Project No. MAT92-884).

[1] P. Bak, C. Tang, and K. Wiesenfeld, *Phys. Rev. Lett.* **59**, 381 (1987).

[2] Experimental data were originally given by B. Gutenberg and C. F. Richter, *Ann. Geophys.* **9**, 1 (1956). An analysis in terms of SOC can be found, for example, in Z. Olami, H. J. S. Feder, and K. Christensen, *Phys. Rev. Lett.* **68**, 1244 (1992).

[3] K. L. Babcock and R. M. Westervelt, *Phys. Rev. Lett.* **64**, 2168 (1990); X. Che and H. Suhl, *Phys. Rev. Lett.* **64**,

1670 (1990).

[4] P. J. Cote and L. V. Meisel, *Phys. Rev. Lett.* **67**, 1334 (1991); L. V. Meisel and P. J. Cote, *Phys. Rev. B* **46**, 10822 (1992).

[5] M. Bretz, J. B. Cunningham, P. L. Kurczynski, and F. Nori, *Phys. Rev. Lett.* **69**, 2431 (1992); G. A. Held, D. H. Solina, D. T. Keane, W. J. Haag, P. M. Horn, and G. Grinstein, *Phys. Rev. Lett.* **65**, 1120 (1990).

[6] P. Diodati, F. Marchesoni, and S. Piazza, *Phys. Rev. Lett.* **67**, 2239 (1991).

[7] G. Cannelli, R. Cantelli, and F. Cordero, *Phys. Rev. Lett.* **70**, 3923 (1993).

[8] A. G. Kachaturyan, *Theory of Structural Transformations in Solids* (Wiley, New York, 1983).

[9] Ll. Mañosa, A. Planes, D. Rouby, M. Morin, P. Fleischmann, and J. L. Macqueron, *Appl. Phys. Lett.* **54**, 2574 (1989).

[10] Z. Yu and P. C. Clapp, *J. Appl. Phys.* **62**, 2212 (1987); Ll. Mañosa, A. Planes, D. Rouby, and J. L. Macqueron, *Acta Metall. Mater.* **38**, 1635 (1990).

[11] E. Vives, J. Ortín, Ll. Mañosa, I. Ràfols, R. Pérez-Magrané, and A. Planes (to be published).

[12] We have performed experiments with heating and cooling rates ranging from  $0.1 \text{ K min}^{-1}$  up to  $2 \text{ K min}^{-1}$ . They have shown that, within this range, our results are not influenced by the heating/cooling rate.

[13] J. Baram and M. Rosen, *Acta Metall.* **30**, 655 (1982).

[14] It has been computed using a  $5 \mu\text{s} \times 0.05 \text{ mV}$  grid, and the resulting contour levels have been plotted from 0.5 up to 6 average counts per grid cell with a 0.5 spacing.

[15] The value  $B \approx 1$ , given in Ref. [2], corresponds to the distribution of events with energy greater than  $E$ ,  $N(E_0 > E) \sim E^{-B}$ ; the latter can be related to our amplitude distribution assuming  $E \sim A^2$ , giving  $\alpha = 2B + 1$ .

[16] A. Sornette and D. Sornette, *Europhys. Lett.* **9**, 197 (1989).

[17] S. P. Obukhov, *Phys. Rev. Lett.* **65**, 1395 (1990).

[18] This value of  $\tau$  corresponds to the distribution of times between avalanches.

[19] P. Bak and H. Flyvbjerg, *Phys. Rev. A* **45**, 2192 (1992).

[20] J. V. Andersen and O. G. Mouritsen, *Phys. Rev. A* **45**, R5331 (1992).

[21] J. P. Sethna, K. Dahmen, S. Kartha, J. A. Krumhansl, B. W. Roberts, and J. D. Shore, *Phys. Rev. Lett.* **70**, 3347 (1993).

[22] J. Ortín, *J. Appl. Phys.* **71**, 1454 (1992), and references therein.

[23] C. Auguet, E. Cesari, and Ll. Mañosa, *J. Phys. D* **22**, 1712 (1989); C. Picornell, C. Seguí, V. Torra, and R. Rappacioli, *Scr. Metall.* **22**, 999 (1988).

[24] S. L. Miller, W. M. Miller, and P. J. McWorter, *J. Appl. Phys.* **73**, 2617 (1993).

[25] D. Sornette, *J. Phys. I* (France) (to be published).

[26] B. J. West and M. F. Shlesinger, *Int. J. Mod. Phys. B* **3**, 795 (1989); *Am. Sci.* **78**, 40 (1990).

[27] E. Hornbogen, *Z. Metallkde.* **78**, 352 (1987); K. Kindo, K. Hazumi, and M. Date, *J. Phys. Soc. Jpn.* **57**, 715 (1988); Q. Y. Long, Y. H. Wen, Z. Zhu, X. M. Zhang, Z. Q. Mu, and C. W. Lung, *Philos. Mag.* **68**, 885 (1993).

[28] J. L. Macqueron (private communication).

[29] A. Amengual, F. Garcías, F. Marco, C. Seguí, and V. Torra, *Acta Metall.* **36**, 2329 (1988).